ELSEVIER

Journal of Nuclear Materials 290–293 (2001) 341–345

journal of nuclear materials

www.elsevier.nl/locate/jnucmat

Erosion and deposition effects on the vessel wall of TEXTOR-94

J. von Seggern [a,*], M. Mayer [a], D. Reiser [a], M. Rubel [b], V. Philipps [a]

[a] *Institute of Plasma Physics, Research Centre Jülich, EURATOM Association, Trilateral Euregio Cluster, D-52425 Jülich, Germany*
[b] *Alfvén Laboratory, Royal Institute of Technology, Association EURATOM-NFR, S-10044 Stockholm, Sweden*

Abstract

Two different sets of long term samples (LTS) were exposed in TEXTOR-94 at the liner with boronized and siliconized wall conditions. Measured erosion/deposition rates of the coating constituents were compared with sputtering rates calculated for pure elements. D^0-fluxes at the LTS locations were determined by the B2-EIRENE code. Over the whole liner, erosion of initial coatings by D^0 is observed. Boron erodes at a rate of 8.4×10^{13} B cm^{-2} s^{-1}, while silicon erodes at a rate of 5.6×10^{13} Si cm^{-2} s^{-1}, a factor of 1.5 lower than that of boron. With boronized walls, carbon atoms initially present in the a-C/B:D layers are eroded at a rate of 7.6×10^{12} C cm^{-2} s^{-1}, at the same time 1.7×10^{12} (Fe + Cr + Ni) cm^{-2} s^{-1} are deposited. Compared to boronized conditions where carbon erodes, deposition of carbon (1.7×10^{13} cm^{-2} s^{-1}) and of metals (3.8×10^{12} cm^{-2} s^{-1}) occurred during the Si campaign. Due to long time exposure at high wall temperature (350°C), hydrogenic isotopes desorb; (D + H)/(B + C) and (D + H)/(Si + C) ratios degrade from originally ~0.4 to ~0.2.

Keywords: TEXTOR 94; Plasma facing materials; Erosion; Deposition; Boron; Carbon; Silicon; Hydrogen; Deuterium

1. Introduction

In tokamak devices, the surface composition of the first wall is determined by the conditioning and operational history of the machine. Aside from sputtering by ions, all areas of the plasma facing components (PFC) are bombarded with energetic neutrals created predominantly in charge-exchange (CX) collisions [1,2]. Both sputtering of plasma limiting components by incident ions, and sputtering of the vessel wall areas by energetic neutrals are dominant sources of impurities transported throughout the machine.

Since the total flux of CX-neutrals at the wall components is of the order of 10^{15} particles cm^{-2} s^{-1}, erosion by hydrogenic neutrals is the dominant mechanism at wall areas not hit by ions from the plasma [2–4]. Additionally, D_2 and He glow discharge cleaning between plasma operations leads to a pronounced erosion of the vessel components. Moreover, CX-neutrals affect the inventory of hydrogenic species in the wall. Material removed at one location is transported in the scrape-off layer and deposited at obstacles present in the machine. It can form, also on areas far from the last close flux surface (LCFS), several 100 μm thick, flaking, differently structured deposits [5–10]. Generally, the location of erosion differs from that of the redeposition.

One of the critical issues for the choice of the vessel wall materials for future fusion devices like ITER is the erosion behavior of the PFCs. To predict the erosion rate and the transport of eroded particles to other locations, a detailed knowledge about erosion mechanism is required. Hence, quantification and global description of the production of impurities and their redeposition at different areas of the vessel will be presented.

2. Experimental

Because of relatively low particle fluxes close to the vessel wall, reasonable measurements are only possible

* Corresponding author. Tel.: +49-2461 61 5623; fax: +49-2461 61 2660.
E-mail address: j.von.seggern@fz-juelich.de (J. von Seggern).

0022-3115/01/$ - see front matter
PII: S0022-3115(00)00635-8

using long term samples (LTS) exposed throughout whole the experimental campaigns. Two operational campaigns were used for long term erosion/deposition studies in TEXTOR-94. Batches of LTS have been installed directly at the inner wall (liner) at a radius of 55 cm. Due to the good thermal contact of the liner, the temperature of the LTS can be taken to be the regular one of the liner vessel (350°C). Though the LTS have had an undisturbed line-of-sight to the plasma, they were protected by limiters (toroidal belt limiter ALTII, main poloidal limiters, and inner bumper limiter) against direct plasma contact. TEXTOR-94 was operated at different line averaged plasma densities ranging between 1.5×10^{13} and 6×10^{13} cm^{-3}, the plasma current was typically 350 kA, and the toroidal magnetic field 2.25 T. Neutral beam injectors (2) supply up to 1.5 MW per injector and ICRH up to 1.3 MW per antenna (2). TEXTOR-94 was operated predominantly with D_2 fuelled plasma discharges with a minor plasma radius of 46 cm.

For characterisation of the layers deposited during boronizations with deuterated diborane or siliconizations using deuterated silane, additional targets were exposed to the conditioning procedures. They were removed from TEXTOR-94 directly after conditioning and examined by electron probe microanalysis (EPMA), elastic recoil detection analysis (ERDA), nuclear reaction analysis (NRA), thermal desorption spectroscopy (TDS), ellipsometry, and by sputter Auger electron spectroscopy (AES).

During the operational campaign August–December 1997 16 LTS holders equipped with Si ⟨111⟩, Inconel 625 and graphite samples were mounted at different toroidal positions 45° below the inner equator, about 10° below the lower edge of the inner bumper limiter (ix 20 in Fig. 1). During the operation, all the samples have sustained the same treatment as the wall. 1600 discharges, ohmic and auxiliary heated, with a total discharge time of about 7620 s were performed. Additionally, two boronizations as well as periodic discharge cleaning procedures in deuterium followed by discharges in helium occurred. The second long term experiment took place between March and July 1999. Again a batch of 16 LTS holders equipped with polished Si, Inconel, and graphite samples was attached to the liner. Eight of the fitted holders were joined, as previously, at the bottom 45° below the equator (further called bottom), the other eight holders were mounted at the top of the machine (ix 49 in Fig. 1). In toroidal direction, the holders alternated between top and bottom positions. During this campaign, two siliconizations and 1430 plasma discharges mainly in D_2, ohmic and auxiliary heated by NBI and ICRH, with a total discharge time of 6600 s were performed.

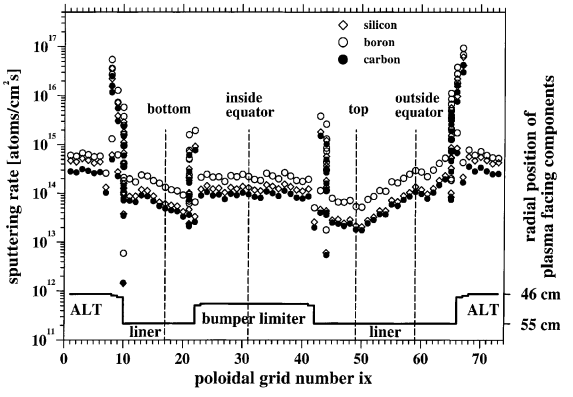

Fig. 1. Poloidal distribution of physical sputtering rates of silicon, boron and carbon by D^0 at TEXTOR-94 liner radius [14]. The poloidal coordinate ix refers to the calculation grid of the B2-EIRENE code [13].

16 toroidal positions distributed alternatively over two poloidal locations within the torus allowed to analyse latent poloidal as well as toroidal variation of the erosion/deposition behavior of the liner wall. After dismounting, the LTS were analysed by ion beam techniques (NRA, ERDA), TDS, EPMA, and by sputter AES. The thickness and optical constants of the layers were determined by ellipsometry.

3. Results and discussion

3.1. Particle fluxes and sputtering rates

Ions flowing along the magnetic field lines of the plasma are the primary source of particles which erode the limiters defining the LCFS. Major erosion is observed at the plasma exposed faces of the limiters [11,12]. After hitting the limiter surfaces, the ions recycle as low energetic neutral particles back into the plasma and collide with incoming, high energetic ions in CX collisions. This creates fast neutral particles, which dominate the erosion at the vessel wall.

Particle fluxes of CX-neutrals with energy and angular distribution $\Gamma = \Gamma(E, \theta)$ have been calculated for a typical TEXTOR ohmic shot (350 kW, $n_e = 3.5 \times 10^{13}$ cm^{-3}) using the B2-EIRENE code [13]. The integral energy distribution for each wall segment $\Delta\theta$ and each energy interval ΔE on a logarithmic scale used in the calculation is defined as $\tilde{\Gamma}(E, \theta) = \frac{1}{\Delta\theta} \int_{\Delta\theta} \int_{\Delta E} \Gamma(E, \theta)\, dE\, d\theta$. The energy distribution of the neutrals is broad, varying from a few eV up to several keV. The maximum particle flux Γ appears at about 100 eV. The total particle fluxes impinging the wall at poloidal positions occupied by the LTS are 2.1×10^{15} at the top and 4.7×10^{15} D cm^{-2} s^{-1} at the bottom.

Sputtering rates have been calculated for different materials at normal incidence applying the modified

Bohdansky formula using parameters from [14] and the incident D^0-fluxes provided by the B2-EIRENE code. For carbon, only physical sputtering was taken into account. Fig. 1 shows the poloidal distribution of the sputtering rates of Si, B, and C at the outer calculation boundary of the B2-EIRENE code representing the vessel wall. The largest rates are observed at the edges of the ALT-II and the inner bumper limiters. It is due to a high production of CX-neutrals generated by large particle fluxes to the edges of the limiter tiles. At these points, the magnetic field lines hit the limiters at an angle of about 8°. The incident high ion fluxes result in a high flux of recycling D^0 inducing a large flux of energetic CX-neutrals. This leads, consequently, to an enhanced sputtering rate. Besides these edges, large sputtering rates are noticed at the surface of the ALT-II limiter and at the surface of the inner bumper limiter. The erosion of boron is generally higher than that of silicon. Carbon shows the lowest erosion. However, it should be kept in mind that only physical sputtering of carbon was taken into account. Due to the additional contribution of chemical erosion by the formation of methane, the total carbon erosion is considerably larger.

3.2. Long term behavior of the vessel wall

During the first long term exposure with boronized wall conditions, two boronizations were performed (exposure no.1). By the boronizations 9.9×10^{17} B cm^{-2}, 1.7×10^{17} C cm^{-2}, and 5.8×10^{17} D cm^{-2} were deposited in the form of an approximately 220 nm thick a-B/C:D coating. By two siliconizations (exposure no. 2), a $\sim$250 nm thick a-Si:D layer consisting of 9.5×10^{17} Si cm^{-2} and 4.2×10^{17} D cm^{-2} was formed. Additionally, 0.2×10^{17} C cm^{-2} were incorporated at the interfaces. In both cases, the D/(B + C) or D/Si ratio was between 0.4 and 0.5, ratios typical for this type of conditioning layers.

The LTS exposed in the boronized machine to discharges at the bottom show pronounced erosion of the original coating. However, deposition of Fe, Ni and some Cr is also observed. The toroidal distribution of the erosion/deposition is shown in Fig. 2. The figure displays also the expected B and C erosion calculated from the D^0-fluxes in a typical TEXTOR ohmic shot at the poloidal position of the LTS as dashed (boron) and dotted line (carbon), respectively. The calculated sputtering rates of pure elements are here multiplied by factors representing the composition of the original coating (0.8B + 0.2C). The data illustrate that the average value of the erosion measured at one poloidal position over the whole toroidal direction is within a factor of $\sim$2 in good agreement with the calculated data. Metals deposited on the LTS may originate from areas at which the conditioning layer is lacking, damaged, e.g., by arcing and disruptions. The relative concentration of

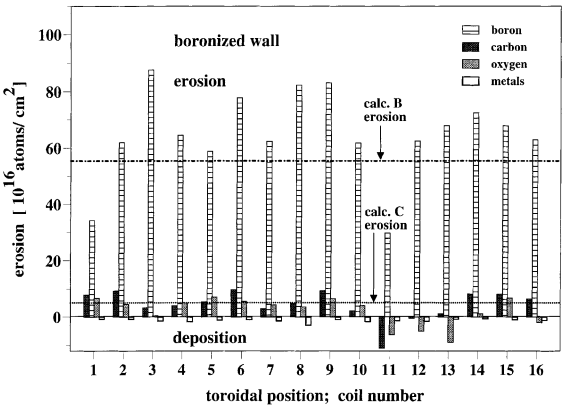

Fig. 2. Toroidal distribution of the total erosion/deposition of the wall components at liner radius of the boronized TEXTOR-94.

Ni:Cr:Fe in this deposit is about 0.5:0.2:0.3, with some similarity to the composition of the Inconel wall (Ni:Cr:Mo:Fe = 06:0.2:0.1:0.05) but with an excess of Fe and none Mo. Except two toroidal positions (coils 1 and 11), the observed erosion and deposition shows only small toroidal variations. Plain graphite test limiters are often used in sector 10/11. They provide an additional source of sputtered C which might deposit at adjacent regions, as is suggested from the carbon deposition on the LTS at coil 11, see Fig. 2.

In the second long term exposure (siliconized walls), the LTS were coated with layers essentially free of carbon. As mentioned above, carbon is located exclusively at the interfaces, the C/Si ratio is around 0.02. The measured erosion/deposition in the second long term exposure is shown in. Fig. 3. Since at the same toroidal position only small difference of the erosion/deposition between the two poloidal locations was observed, the data yielded from the top and bottom of the device were

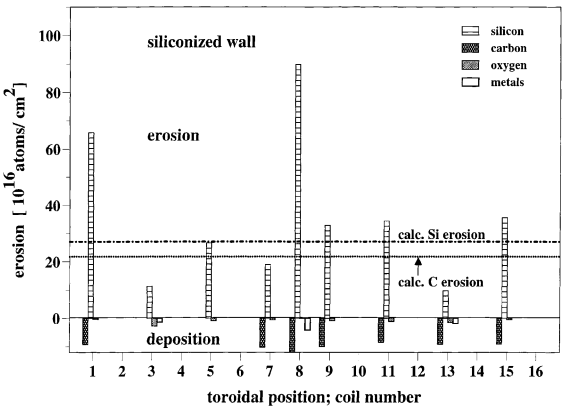

Fig. 3. Toroidal distribution of the total erosion/deposition of the wall components at liner radius of the siliconized device.

Table 1
Calculated and measured mean erosion and deposition rates of B, Si, C, metals, and D in boronized and siliconized TEXTOR-94

Material	Calculated sputtering rates (atoms cm^{-2} s^{-1})	Boronized TEXTOR-94 (atoms cm^{-2} s^{-1})		Siliconized TEXTOR-94 (atoms cm^{-2} s^{-1})	
		Mean erosion rate	Mean deposition rate	Mean erosion rate	Mean deposition rate
Boron	9.1×10^{13}	8.4×10^{13}	–	–	–
Silicon	4.1×10^{13}	–	–	5.6×10^{13}	–
Carbon	3.3×10^{13}	7.6×10^{12}	–	–	1.7×10^{13}
Iron + Nickel	–		1.7×10^{12}	–	3.8×10^{12}
Deuterium	–	5.1×10^{13}	–	5.8×10^{13}	–

averaged. At all toroidal positions, the a-Si:D coating is eroded, with a minimum erosion of about 1×10^{17} Si cm^{-2} at coil no. 13 and a maximum erosion of about 9×10^{17} Si cm^{-2} at coil no. 8. Despite the observed Si erosion, however, a net carbon deposition, spread over the whole torus, took place. The mean C/Si ratio increased from the initial value of 0.02 directly after the siliconizations to a value of 0.6 in the films modified by the plasma. As proven by depth profiles measured by sputter AES, the carbon is concentrated at the top of the eroded initial coatings. This carbon originates from the graphite limiters; fractions of conditioning films deposited upon the limiters erode within only a few plasma discharges, and uncovered, original limiter surfaces emerge. However, only a small part of the C atoms sputtered from the limiters reaches the outer wall. Except 2 positions (coils no. 1 and 8), the calculated Si erosion is in a good agreement with the measured one. The enhanced erosion at these positions is not clarified yet. As in the prior experiment, metals eroded from the bare, destroyed areas of the wall are transported through the machine and deposited, among other places, at the liner surface.

A summary of the erosion/deposition performance of both wall conditionings are presented in Table 1. Integrating the erosion rates over the entire area of TEXTOR-94 liner (3×10^5 cm^2) 2.5×10^{19} B s^{-1} and 1.7×10^{19} Si s^{-1} erode in the plasma discharge. Total sputtering rates of B, Si, and C calculated for incident (D^0)-fluxes at the locations of the LTS are also shown. The energy distribution of the impinging neutrals have been taken into account. Due to the lower Si-sputtering rates (Fig. 1), siliconized walls erode slower than boronized ones, the erosion of siliconized walls proceeds a factor of ~0.6 slower than the destruction of the walls under boronized conditions. The a-Si:D coatings protect the first wall more efficiently. As mentioned above, the net erosion of carbon in the machine coated with a-C/B:D turns to the net carbon deposition in the siliconized, initially carbon free device. The deposition of metals in the siliconized machine is a factor of about two higher than that in a machine with boronized walls. However, this may be caused by some higher number of local destroying events during the campaign with siliconized vessel.

During the long time operation, the walls lose to some extent deuterium initially present in the conditioning layers. Deuterium inventory reached values between 5×10^{15} cm^{-2} at the high erosion area and 1×10^{17} cm^{-2} at the low one. Additionally, a significant amount of protium is observed in the deposited layer [15]. High amount of protium providing a H/D ratio of ~2 have been found by ERDA and NRA. Occasional discharges in hydrogen, neutral beam injections of hydrogen, and certain H_2O uptake from air moisture during storage in air may support both the hydrogen implantation and the isotope exchange in the film. The ratios of (D + H)/(B + C) and (D + H)/(Si + C) after the exposure is ~0.2. Compared to virgin deposits with a ratios of 0.4–0.5, a reduction of a factor of ~2 occurs. The depletion of the (D + H) value in these films is mostly due to thermal desorption by the long term operation of TEXTOR at the wall temperature of 350°C. As measured by TDS, the desorption of D and H exhibits a broad maximum, starting already at about 200°C.

4. Summary

Erosion and deposition effects at the liner wall of TEXTOR-94 have been studied under boronized and siliconized wall conditions by two sets of LTS. The measured erosion/deposition rates of the coating constituents were compared with sputtering rates calculated for pure elements. The D^0-fluxes and their energy distribution at the LTS locations were determined by the B2-EIRENE code.

Over the whole liner, a pronounced erosion of the initial conditioning coatings by CX-neutrals is observed. According to the calculations, the total D^0-fluxes in ohmic discharges ($n_e = 3.5 \times 10^{13}$ cm^{-3}) at the LTS positions are up to 4.7×10^{15} D cm^{-2} s^{-1}. Boronized walls erode a factor of ~1.5 faster than the siliconized ones. The measured erosion is in good agreement with calculated values. Carbon as a component of the

a-C/B:D films erodes together with boron. Initially carbon free siliconization layers display pronounced net deposition of C. Additionally, deposition of metals on top of the coatings was seen.

During the exposure, coatings lost deuterium but incorporated a substantial quantity of protium. However, a depletion of hydrogenic species in the coatings was observed.

References

[1] R. Behrisch, J. Roth, G. Staudenmaier, H. Verbeek, Nucl. Instr. and Meth. B 18 (1987) 629.
[2] V. Verbeek, G. Stober, D.P. Coster et al., Nucl. Fus. 38 (1998) 1789.
[3] G. McCracken, Plasma Phys. Control. Fus. 29 (1987) 7.
[4] J. Roth, G. Jahneschitz, Nucl. Fus. 29 (1989) 915.
[5] J.P. Coad, B. Farmery, Vacuum 45 (1994) 435.
[6] M. Mayer, R. Behrisch, K. Plamann et al., J. Nucl. Mater. 266–269 (1999) 604.
[7] A. Tobasso, J. Roth, H. Mayer et al., in: Proceedings of the 26th EPS Conference on Controlled Fusion and Plasma Physics, vol. 23J, Maastricht, Netherlands, 1999, p. 1533.
[8] M. Mayer, R. Behrisch, P. Andrew et al., Phys. Scr. T 81 (1999) 13.
[9] J. von Seggern, M. Rubel, P. Karduck et al., Phys. Scr. T 81 (1999) 31.
[10] P. Wienhold, D. Hildebrandt, A. Kirschner et al., in: Proceedings of the 10th Toki Conference.
[11] P. Wienhold, F. Weschenfelder, J. von Seggern et al., J. Nucl. Mater. 241–243 (1997) 804.
[12] A. Pospieszczyk, V. Philipps, E. Casarotto et al., J. Nucl. Mater. 241–243 (1997) 833.
[13] D. Reiter, J. Nucl. Mater. 196–198 (1992) 80.
[14] W. Eckstein, C. García-Rosales, J. Roth, W. Ottenberger, Technical Report IPP 9/82, Max-Planck-Institut für Plasmaphysik, Garching, 1993.
[15] M. Mayer, V. Philipps, P. Wienhold et al, these Proceedings.